Sustainable Chemistry and Pharmacy 15 (2020) 100196

Contents lists available at ScienceDirect

Sustainable Chemistry and Pharmacy

journal homepage: http://www.elsevier.com/locate/scp

Pterocarpus santalinoides leaves extract as a sustainable and potent inhibitor for low carbon steel in a simulated pickling medium

Cornelius C. Ahanotu [a], Ikenna B. Onyeachu [b], Moses M. Solomon [b,*], Ikechukwu S. Chikwe [a], Oluchukwu B. Chikwe [c], Chinenye A. Eziukwu [d]

[a] Department of Science Laboratory Technology, Imo State Polytechnic, Umuagwo-Ohaji, Owerri, Nigeria
[b] Center of Research Excellence in Corrosion, Research Institute, King Fahd University of Petroleum and Minerals, Dhahran, 31261, Saudi Arabia
[c] Department of Pure and Industrial Chemistry, Nnamdi Azikiwe University, Awka, Nigeria
[d] Department of Chemistry, Edo University, Iyamo, Edo State, Nigeria

ARTICLE INFO

Keywords:
Pterocarpus santalinoides
Extractive solvent
Acid corrosion
Inhibition
Adsorption

ABSTRACT

The crude extract of *Pterocarpus santalinoides* leaves (PSLE) extracted using water, ethanol, and methanol as the extraction solvent has been studied as inhibitor for low carbon steel in 1 moL/dm^3 HCl solution using electrochemical approaches at 25 °C and 60 °C. The results obtained reveal that, PSLE extract has the capacity to effectively suppress the dissolution of the studied substrate. The inhibition performance of PSLE is a function of concentration, temperature, and extraction solvent. Corrosion inhibition is in the order: ethanolic extract > methanolic extract > aqueous extract. With 0.7 g/L PSLE, inhibition efficiency of >90% has been obtained at 60 °C. Based on calculated values of adsorption parameters and UV–vis results, it is proposed that PSLE molecules chemically interacted with the substrate surface. PSLE extract suppressed both the rate of cathodic and anodic reactions according to the PDP results. However, aqueous PSLE extract inhibited anodic corrosion reactions predominantly while ethanolic and methanolic extracts mainly inhibited the cathodic corrosion reactions. Surface characterization studies via SEM, EDAX, and AFM provide experimental evidence to the claim of interaction and presence of PSLE molecules on the studied substrate surface.

1. Introduction

Metals are critical to industrial development. Many industrial equipment, transmission lines, and storage facilities are fabricated from metals. From time to time, the industrial cleaning of metallic equipment is necessary to get rid of fouling, prevent damage, and maintain efficiency of operation. One of the efficient cleaning procedures is chemical cleaning, which uses mostly inorganic or organic acid solution as the cleaning solution (Otzisk, 2008). For the removal of inorganic scales, common cleaning solution is inhibited inorganic acids (HCl, H_2SO_4, H_3PO_4) in the concentration range of 2–5% and temperature less than 60 °C (Otzisk, 2008). Inhibitors for chemical cleaning process are mostly organic compounds having S, N, O heteroatoms and/or π electrons in their molecules (Noor, 2005; Kannan et al., 2016; Tuken et al., 2012; Zhang and Hua, 2009).

Although the organic corrosion inhibitors have been effective, the synthesis routes of some of them are rigorous and some are very expensive. Additionally, some organic inhibitors possess high toxicity and are unhealthy to humans and the natural environment (Fang et al., 2019). As an alternative to the toxic organic inhibitors, compounds such as the natural polymers, amino acids, ionic liquids, and plant extracts, that are less harmful to humans and the natural environments have been advocated for use as metals corrosion inhibitors (Fang et al., 2019; Solomon et al., 2018; Obot et al., 2017; Kannan et al., 2016; Ashassi--Sorkhabi et al., 2004). Among these green compounds, plant extract has received the most research attention owing to its availability and low cost (Fang et al., 2019; Alibakhshi et al., 2019; Sanaei et al. 2019).

Research findings have shown that extracts from different plant parts are effective in retarding metals corrosion in hostile environments (Table 1). As could be seen in Table 1, corrosion inhibition efficiency greater than ninety percent is achievable with plant biomaterials. The performance of plant extracts as corrosion inhibitors is due to the presence of complex organic molecules in their composition (Umoren et al. 2019; Mobin et al., 2019). The heteroatoms (N, S, and O), the conjugated double/triple bonds, as well as the aromatic rings in the molecular structures of the organic compounds serve as the interaction

* Corresponding author.
E-mail address: moses.solomon@kfupm.edu.sa (M.M. Solomon).

https://doi.org/10.1016/j.scp.2019.100196
Received 23 September 2019; Received in revised form 31 October 2019; Accepted 30 November 2019
Available online 5 December 2019

Table 1
Some recent studies on plant biomaterials as inhibitor for low carbon steel under acid cleaning conditions.

Plant name	Plant part extracted	Extraction solvent	Corrodent studied	Optimum η (%)	Optimum concentration	Ref.
Saraca ashoka	Seed	Ethanol	H_2SO_4	95.48	100 mg/L	Saxena et al., 2018a
Cuscuta reflexa	Fruit	Ethanol	H_2SO_4	95.47	500 mg/L	Saxena et al., 2018b
Myristica fragrans	Fruit	Ethanol	H_2SO_4	87.81	500 mg/L	Haldhar et al. (2018a)
Armoracia rusticana	Root	Ethanol	H_2SO_4	95.74	100 mg/L	Haldhar et al. (2018b)
Ficus religiosa	Fruit	Ethanol	H_2SO_4	92.26	500 mg/L	Haldhar et al. (2018c)
Aegle marmelos	Fruit	Ethanol	H_2SO_4	83.08	500 mg/L	Bhardwaj et al. (2018)
Asparagus racemosus	Fruit	Ethanol	H_2SO_4	93.25	100 mg/L	Saxena et al., 2018c
Ficus tikoua	Leaf	Water	HCl	95.80	200 mg/L	Wang et al. (2019)
Pineapple	Stem	–	HCl	97.60	1000 ppm	Mobin et al. (2019)
Eriobotrya japonica Lindl	Leaf	Water	HCl	92.70	800 ppm	Nikpour et al. (2019)
Lemon Balm	–	Water	HCl	94.60	800 ppm	Asadi et al. (2019)
Rosa canina	Fruit	Water	HCl	85.35	800 ppm	Sanaei et al. (2019)
Peganum harmala	Seed	Water	HCl	95.00	600 ppm	Bahlakeh et al., 2019a
Petroselium sativum	Leaf	HCl	HCl	92.39	5 g/L	Benarioua et al. (2019)
Mustard	Seed	Water	HCl	94.00	200 mg/L	Bahlakeh et al. (2019b)
Chinese gooseberry	Fruit	Water	HCl	91.90	1000 ppm	Dehghani et al. (2019c)
Citrullus lanatus	Fruit	Water	HCl	91.00	800 mg/L	Dehghani et al. (2019d)
Borage	Flower	Water	HCl	91.00	800 mg/L	Dehghani et al. (2019a)

η = inhibition efficiency.

centers between plant extracts and metallic surfaces (Mobin et al., 2019). A comprehensive information on plant extracts as metals corrosion inhibitor can be found in Umoren et al. (2019).

Pterocarpus santalinoides is a tree of about 9–12 m high that belongs to the legume family of *Fabaceae*. It is native to the tropical Western Africa (World Agroforestry Centre, 2008). Traditionally, the leaves are used in the treatment of skin diseases such as eczema, candidiasis and acne (Osuagwu and Akomas, 2013). The bark extracts have been applied for the treatment of diabetes, cough and sore belly (Igoli et al., 2005; Okwuosa et al., 2011). It was reported that *Pterocarpus santalinoides* leaves extract contained coumarins, polyphenols (flavonoids and tannins), saponins and leucoanthocyanins (Bothon et al., 2014). These phytochemicals are rich in heteroatoms and hence, *Pterocarpus santalinoides* has one of the qualifications required from a potential corrosion inhibitor.

Extract of *Pterocarpus santalinoides* leaves had been studied as mild steel corrosion inhibitor in H_2SO_4 solution and protection efficiency value as high as 96% was reported (Ofoma et al., 2018). However, only the classical chemical techniques (weight loss and gasometric) were used in the investigation. Since aqueous corrosion of metals is an electrochemical reaction involving oxidation and reduction half-reactions occurring, respectively, at anodic and cathodic sites on the metal surface, it is pertinent to understand how *Pterocarpus santalinoides* leaves extract modifies these reactions during the acid corrosion of carbon steel. The rationale for such investigation is also emphasized by the general acceptance that organic inhibitors inhibit corrosion by adsorptive mechanism or by increasing the electrical resistance of a substrate surface (Fang et al., 2019).

In this report, we used the electrochemical techniques to study the extent of protection of a low carbon steel against dissolution in a molar hydrochloric acid solution at 25 and 60 °C by *Pterocarpus santalinoides* leaves extract. To assess the contribution of extraction solvent to inhibition performance of the extract, different extractive solvents (ethanol, water, and methanol) were used in the extraction process.

2. Experimental section

2.1. Materials and solutions

Fresh *Pterocarpus santalinoides* leaves (PSLE) were collected from the campus of Imo State Polytechnic, Umuagwo-Ohaji, Owerri, Nigeria and was validated by Dr. B. E. Onwubuche of the Department of Plant Science and Technology, Imo State Polytechnic, Nigeria. The leaves were washed thoroughly with distilled water, sun dried for two weeks, and then ground into powder. For extracting and processing, 10.0 g PSLE powder was soaked in 800 mL of extracting solvent (ethanol, methanol or water) for 24 h. Thereafter, the mixture was filtered and the filtrate was concentrated utilizing a rotary evaporator. In each case, extract in the range of 1.34–1.37 g was obtained. The plant leaves extract was characterized using a Fourier-transform infrared spectroscopy (FTIR) spectrophotometer (Nicolet iS5, Thermo Scientific model) over the range 4000 to 400 cm^{-1}.

The chemical composition of the low carbon steel specimens is same as given in Solomon et al. (2017). Circular shaped samples with exposed area of 0.79 cm^2 were used for electrochemical measurements. Before the specimens were used for each experiment, they were abraded, mechanically using abrasive papers with 400–800 grit, rinsed in distilled watere and acetone and dried using a Buchler Torramet specimen dryer. Analytical reagent hydrochloric acid (37%) was dissolved in distilled water to prepare the corrodent (1 moL/dm^3 HCl). In this study, the concentration range of the PSLE extract investigated was 0.1–0.7 g/L.

2.2. Electrochemical experiments

All electrochemical experiments were conducted on a Gamry Potentiostat/Galvanostat/ZRA Reference 600 workstation following the ASTM G3-89 (1994) and G5-94 (1994) standard procedures and utilizing 150 mL as the volume of the test solutions. An epoxy-encapsulated low carbon steel was the working electrode, the auxiliary electrode was a graphite rod, and the reference was a Ag/AgCl electrode. Electrochemical experiments were performed after monitoring the variation of open circuit potential (OCP) for an hour. The electrochemical impedance spectroscopy (EIS) measurements were undertaken at the frequency range of 10^4 Hz to 10^{-3} Hz with a $\pm$ 10 mV amplitude signal and acquirement of 10 points/decade at OCP. Linear polarization resistance (LPR) experiments were performed from −10 mV to +10 mV versus OCP and the scan rate of 0.125 mVs^{-1} was used. Finally, potentiodynamic polarization (PDP) measurements were conducted at the potential of ±0.25 V versus OCP utilizing a scan rate of 0.2 mVs^{-1}. The analysis of EIS and LPR data was done using Echem analyst while EC-lab software was used for PDP data analysis. For reproducibility, all the experiments were repeated three times. The inhibition efficiency from EIS, LPR, and PDP techniques was calculated using equations given elsewhere (Fang et al., 2019; Solomon et al. 2018).

2.3. SEM, EDAX, AFM, and UV–vis experiments

The surface morphologies of the low carbon steel coupons immersed in 1 moL/dm^3 HCl solution without and with 0.7 g/L PSLE extract for 24 h were observed using a scanning electron microscope (SEM), JEOL

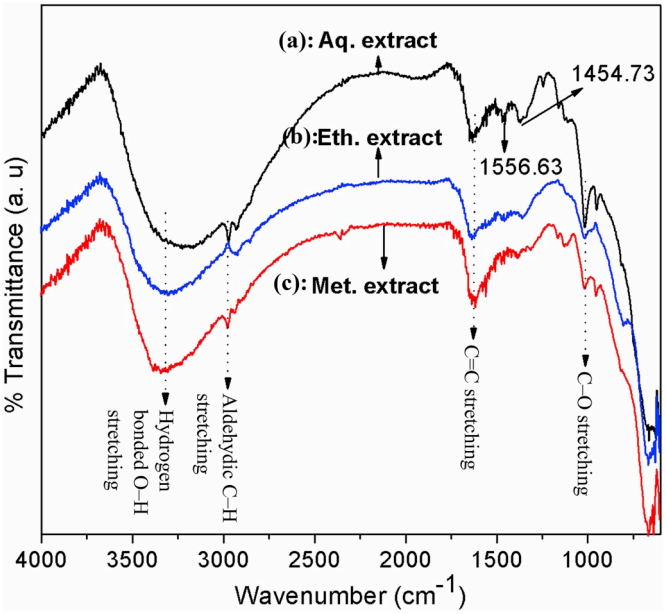

Fig. 1. FTIR spectra of aqueous, methanolic, and ethanolic extract of *Pterocarpus santalinoides*.

JSM-6610 LV model coupled to energy dispersive X-ray spectroscopy (EDAX) for chemical composition determination. AFM measurements were performed using a 5420 atomic force microscope (N9498S, Agilent Technologies, UK) operated in the contact mode under ambient conditions. The ultra violet–visible (UV–vis) experiments were undertaken utilizing a JASCO770-UV–Vis spectrophotometer (200–650 nm) using a dual beam operated at a resolution of 1 nm with a scan rate of 200 nm min^{-1}.

3. Findings and discussion

3.1. Characterization of PSLE extract

Fig. 1 presents the FTIR spectra obtained for the aqueous, methanolic, and ethanolic extract of *Pterocarpus santalinoides*. Inspection of the figure reveals that the three spectra contained similar peaks although with different intensities at wavelength region of 3226–3341 cm^{-1}, 2971–2920 cm^{-1}, 1614–1633 cm^{-1}, and 1016–1017 cm^{-1}. This suggests that the studied solvents extracted phytochemical compounds with similar or same functional groups. Nevertheless, some striking differences can be identified in the figure. For instance, the peaks at 1556.63 cm^{-1} and 1371.20 cm^{-1} in Fig. 1(a) (aqueous extract) are absent in Fig. 1(b and c) (methanolic and ethanolic extract). The weak peak around 976 cm^{-1} in Fig. 1(a and c) is absent in Fig. 1 (b). In addition, the peak around 3226–3341 cm^{-1} is broader in Fig. 1(a) than in Fig. 1(b and c). All these observations suggest some slight differences in the phytochemical compounds extracted by the organic solvents and water.

In the spectra, intense and broad peaks observed at 3226–3341 cm^{-1} are typical stretching of H-bonded O–H (Wang et al., 2019). The bands at around 2971–2920 cm^{-1} are typical of aldehydic C–H stretching (Dehghani et al., 2019c,d). The peaks in the region of 1614–1633 cm^{-1} and 1016–1017 cm^{-1} emanated from the vibrations of C=C and C–O groups, respectively (Dehghani et al., 2019d; Wang et al., 2019). In addition, the weak peaks around 1455 cm^{-1} are associated with –COOH stretching vibration (Dehghani et al., 2019c). These results indicate that chemical compounds in the form of ester, carboxylic acid, and aldehyde are present in PSLE extract. These compounds, which may be saturated or unsaturated, have oxygen heteroatoms in their functional groups, which are the universal features of a traditional corrosion inhibitor.

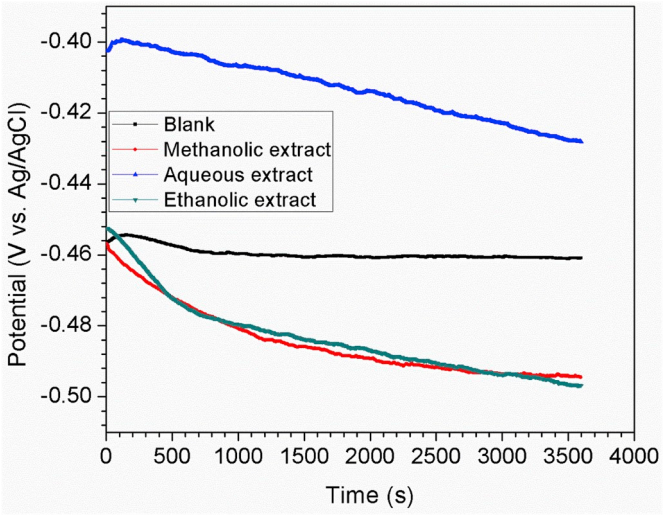

Fig. 2. Representative plots showing the variation of open circuit potential with time for low carbon steel immersed in 1 moL/dm^3 HCl solution without and with *Pterocarpus santalinoides* extract at 25 °C.

3.2. Corrosion inhibition by PSLE extract

3.2.1. OCP studies

The graphs showing the variation of the OCP with immersion duration for the low carbon steel immersed in 1 moL/dm^3 HCl solution unprotected and protected with PSLE extract at 25 °C are shown in Fig. 2. In all cases, an initial rise in open circuit potential (OCP) followed by a decreasing tendency before attaining a steady state condition is observed. This behavior, which had been reported by Chellouli et al. (2016) is linked to the breakdown of the native oxide film on the electrode surface (Zhao et al., 2019; Zohdy, 2015). The oxide film breakdown is followed by the growth of corrosion products (in uninhibited system) and/or adsorbed inhibitor layer (in inhibited system) until a steady state potential is established (Chellouli et al., 2016).

Relative to the blank, it is observed that, the aqueous extract displayed the open circuit potential to nobler values whereas the methanolic and the ethanolic extracts shifted the open circuit potential to more negative values. This is suggestive of different mechanism of inhibition by the extracts. It seems that the aqueous extract affected the anodic corrosion reactions principally while the ethanolic and methanolic extracts influenced the cathodic corrosion reactions more than the anodic reactions. Organic-based inhibitors can retard metals dissolution by interrupting the anodic and/or cathodic corrosion reactions (Sigircik et al., 2016; Srikanth et al., 2007). The classification of an inhibitor as anodic, cathodic, or mixed type requires that, the OCP (inhibited system) minus the OCP (uninhibited system) equals ± 85 mV (Oguzie et al., 2007; Srikanth et al., 2007; Solomon and Umoren, 2016). In this work, the OCP for the low carbon steel in the blank solution at 3600 s is −460.9 mV vs. Ag/AgCl but is −494.5 mV vs. Ag/AgCl, −496.8 mV vs. Ag/AgCl, and −428.0 mV vs. Ag/AgCl, respectively, in the acid solution containing methanolic, ethanolic, and aqueous extract. Since the difference in the OCP of the inhibited and uninhibited solutions is below the benchmark of ±85 mV, PSLE extract is regarded as a mixed type inhibitor.

3.2.2. EIS studies

The impedance response of low carbon steel in 1 moL/dm^3 HCl solution without and with different dosages of PSLE extract has been investigated and the results obtained are presented in Nyquist (Fig. 3 (a–c)), Bode modulus (Fig. 3(d–f)), and Bode Phase (Fig. 3(g–i)) formats. The Nyquist graphs exhibit single capacitive loops at high frequencies and one-time constant is observed in the corresponding Bode

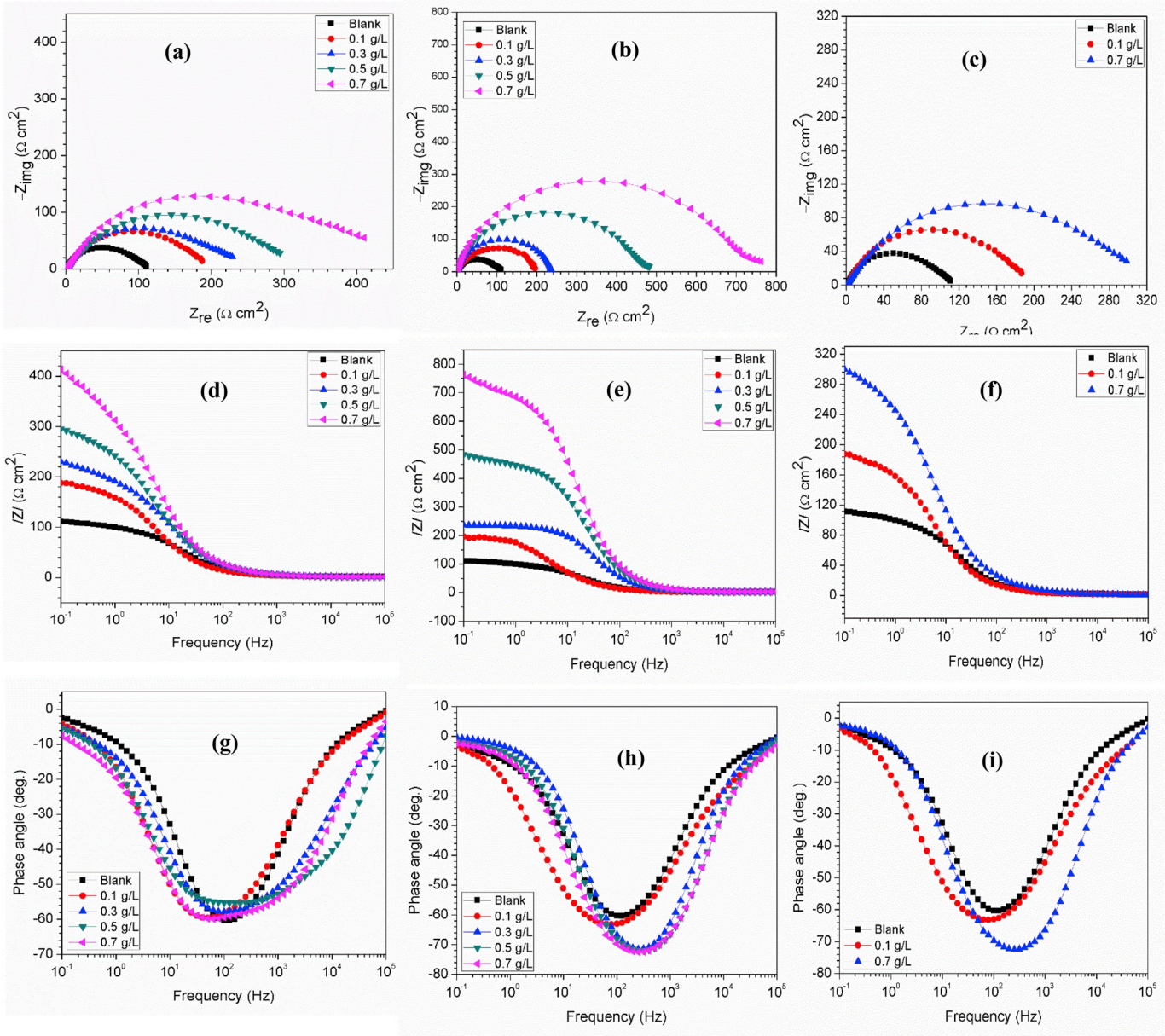

Fig. 3. Electrochemical impedance spectra for low carbon steel in 1 moL/dm^3 HCl solution in the absence and presence of different concentrations of (a, d, g) aqueous, (b, e, h) ethanolic, and (c, f, i) methanolic *Pterocarpus santalinoides* extract at 25 °C.

representations (Fig. 3(d–i)). The observed single capacitive loop indicates that the dissolution of the low carbon steel in the studied medium is controlled primarily by charge transfer process (Zhang and Hua, 2009; Solomon et al., 2018). As should be expected for a solid electrode, the capacitive loops in Fig. 3(a–c) are imperfect and such is often associated with the heterogeneity of the working electrode (Zhang and Hua, 2009; Solomon et al., 2018).

Although the graphs for the uninhibited and inhibited systems are similar, probably due to similar mechanism of corrosion, the influence of the PSLE extract on the corrosion process is obvious. The effect, which is concentration-dependent, is manifested in the larger diameter of the capacitive loops, the displacement of the impedance and the Phase angle to larger values in the extract-inhibited systems relative to the blank. This could be possible due to the obstruction of reaction points on the metal surface by adsorbed inhibitor molecules (Solomon et al., 2017).

The one-time constant observed in Fig. 3 allows the studied system to be described by a simple R(QR) equivalent circuit (EC) inserted in Fig. 4 (a). The suitability of the selected EC is illustrated in Fig. 4. The use of a constant phase element (CPE) in place of a pure capacitor in the EC was necessitated by the depressed nature of the capacitive loops in Fig. 3 (a–c) caused by the heterogeneity of the working electrode (Wang et al., 2019; Sigircik et al., 2016). Mansfeld et al. (1992) recommended the inclusion of n (an exponent) in the impedance function to account for the deviation from an ideal behavior. This recommendation, which has been widely embraced (Fernandes et al., 2019; Ashassi-Sorkhabi et al., 2006), allows the replacement of a pure capacitor with a CPE. The impedance function of a CPE can be described by Eq. (1) (Fernandes et al., 2019; Ashassi-Sorkhabi et al., 2006):

$$Z_{CPE} = Y_0^{-1}(jw)^{-n} \quad (1)$$

where Y_0 = CPE constant, n = CPE exponent, which describes the roughness of a surface and is within the range $-1 \leq n \leq 1$, j = imaginary number ($j = -1)^{1/2}$, while w = angular frequency ($w = 2\pi f$). For a non-ideally polarized electrode where charge transfer controls the corrosion process and diffusion or any other kind of mass transfer is unaccounted

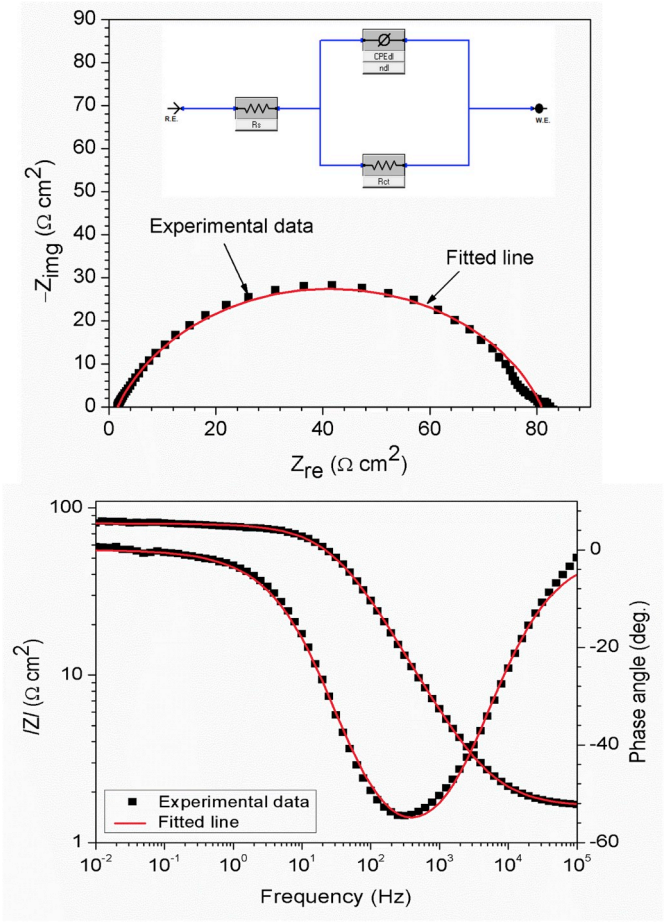

Fig. 4. Experimental and fitted impedance data of low carbon steel in the absence and presence of *Pterocarpus santalinoides* extract. The equivalent circuit used for the fitting is inserted in the Nqyuist representation.

for, the double layer capacitance (C_{dl}) can be computed using the Brug et al. (1984) formula:

$$C_{dl} = Y_0^{1/n}\left(\frac{1}{R_s}+\frac{1}{R_{ct}}\right)^{(n-1)/n} \quad (2)$$

The values of the derived and calculated electrochemical parameters are listed in Table 2. While the value of R_{ct} is observed to be higher in the inhibited systems and increases with increase in PSLE extract concentration, the reverse is noted for the C_{dl}. The highest R_{ct} and the lowest C_{dl} values are noted for 0.7 g/L extract (highest studied concentration). This concentration raised the R_{ct} value from 104.80 ± 0.75 cm^2 to 411.20 ± 3.65 Ω cm^2, 710.50 ± 4.73 Ω cm^2, and 379.40 ± 3.13 Ω cm^2 and decreased the C_{dl} value from 55.20 μF cm^{-2} to 9.68 μF cm^{-2}, 10.40 μF cm^{-2}, and 21.50 μF cm^{-2}, respectively for the aqueous, ethanolic, and methanolic PSLE extract. These observations demonstrate the formation of a protective layer on the low carbon steel surface (Dehghani et al., 2019a-d). This layer boosted the corrosion resistance of the substrate. The inverse variation of the C_{dl} with extract concentration aligned with the Helmholtz model (Fernandes et al., 2019) and depicts a lower local dielectric constant due to the substitution of the adsorbed water molecules on the low carbon steel surface by adsorbed inhibitor molecules (Fernandes et al., 2019; Luo et al., 2019). It means that, the increase in the dosage of the extract increased the thickness of the electrical double layer resulting in a decrease in the surface area exposed to corrosive attack (Fernandes et al., 2019; Luo et al., 2019). The inhibition efficiency afforded by the 0.7 g/L aqueous, ethanolic, and methanolic PSLE extract, respectively is 74.51%, 76.94%, and 72.38%.

3.2.3. PDP studies

Fig. 5 presents the PDP graphs for low carbon steel in 1 moL/dm^3 HCl solution free of and containing different dosages of (a) aqueous, (b) ethanolic, and (c) methanolic PSLE extract at 25 °C. The corresponding polarization parameters obtained from the analysis of the curves are listed in Table 3. The presented results clearly show that, the corrosion of the low carbon steel was retarded by the addition of the plant extract. The addition of 0.1 g/L queous, ethanolic, and methanolic PSLE extract decreased the corrosion current density (i_{corr}) from 124.25 μA cm^{-2} to 71.65 μA cm^{-2}, 68.60 μA cm^{-2}, and 73.41 μA cm^{-2}, respectively and protected the metal surface by 42.33%, 44.79%, and 40.92%. The inhibition becomes better upon increasing the extract concentration probably due to significant adsorption and restriction of dissolution reactions. When the concentration of the aqueous, ethanolic, and methanolic PSLE extract was increased to 0.7 g/L, the i_{corr} further decline to 30.25 μA cm^{-2}, 15.75 μA cm^{-2}, and 33.64 μA cm^{-2}, respectively corresponding to protection efficacy of 75.65%, 79.00%, and 72.93%.

It is observed from Fig. 5 that, the presence of PSLE extract in the corrodent decreases both the anodic and cathodic current densities. In Table 3, it is noticed that, the difference between the anodic and the cathodic slope (β_a and β_c) values of the PSLE-inhibited systems and those of the unprotected is not very significant. These observations indicate that, PSLE extract behaves as a mixed type corrosion inhibitor (Satapathy et al., 2009). However, by finding the difference between the corrosion potential (E_{corr}, blank) and the E_{corr} (inhibited), the ethanolic and methanolic extracts are found to displace the corrosion potential of the steel electrode by 21–47 mV cathodically while the higher concentrations of the aqueous extract shift the potential by 10–12 mV anodically. These results confirm the OCP results (Fig. 2) that the organic solvent extract principally inhibited the cathodic reduction reactions while the aqueous extract predominantly retarded the anodic oxidation reactions.

In a system containing an effective organic corrosion inhibitor, the

Table 2
Electrochemical impedance parameters for low carbon steel in 1 moL/dm^3 HCl solution in the absence and presence of *Pterocarpus santalinoides* extract at 25 °C.

Conc./System	Extracting solvent	R_s (Ω cm^2)	CPE		R_{ct} (Ω cm^2)	x^2 × 10^{-3}	C_{dl} (μF cm^{-2})	η_{EIS} (%)
			Y_0 (μΩ^{-1} s^2 cm^{-2})	n				
Blank	–	1.87 ± 0.01	317.00 ± 0.00	0.81 ± 0.00	104.80 ± 0.75	0.83	55.20	–
0.1 g/L	Aqueous	1.81 ± 0.13	499.20 ± 0.00	0.71 ± 0.00	189.80 ± 1.61	0.74	28.40	44.78
0.3 g/L		1.21 ± 0.12	366.00 ± 0.00	0.72 ± 0.00	227.40 ± 1.85	1.28	18.10	53.91
0.5 g/L		0.73 ± 0.10	431.10 ± 0.00	0.68 ± 0.00	311.80 ± 2.81	1.91	16.50	66.39
0.7 g/L		1.16 ± 0.12	310.10 ± 0.00	0.73 ± 0.00	411.20 ± 3.65	1.60	9.86	74.51
0.1 g/L	Ethanolic	1.17 ± 0.10	475.80 ± 0.00	0.74 ± 0.00	203.40 ± 1.71	1.45	34.10	48.48
0.3 g/L		2.38 ± 0.18	48.59 ± 0.00	0.91 ± 0.00	231.70 ± 1.42	0.19	19.80	54.77
0.5 g/L		2.56 ± 0.21	39.84 ± 0.00	0.89 ± 0.00	454.50 ± 2.91	0.66	12.80	76.94
0.7 g/L		3.04 ± 0.10	36.05 ± 0.00	0.88 ± 0.00	710.50 ± 4.73	0.72	10.40	85.25
0.1 g/L	Methanolic	1.28 ± 0.12	787.90 ± 0.00	0.68 ± 0.00	181.10 ± 1.03	2.64	30.50	42.13
0.7 g/L		0.77 ± 0.00	242.20 ± 0.00	0.78 ± 0.00	379.40 ± 3.13	8.22	21.50	72.38

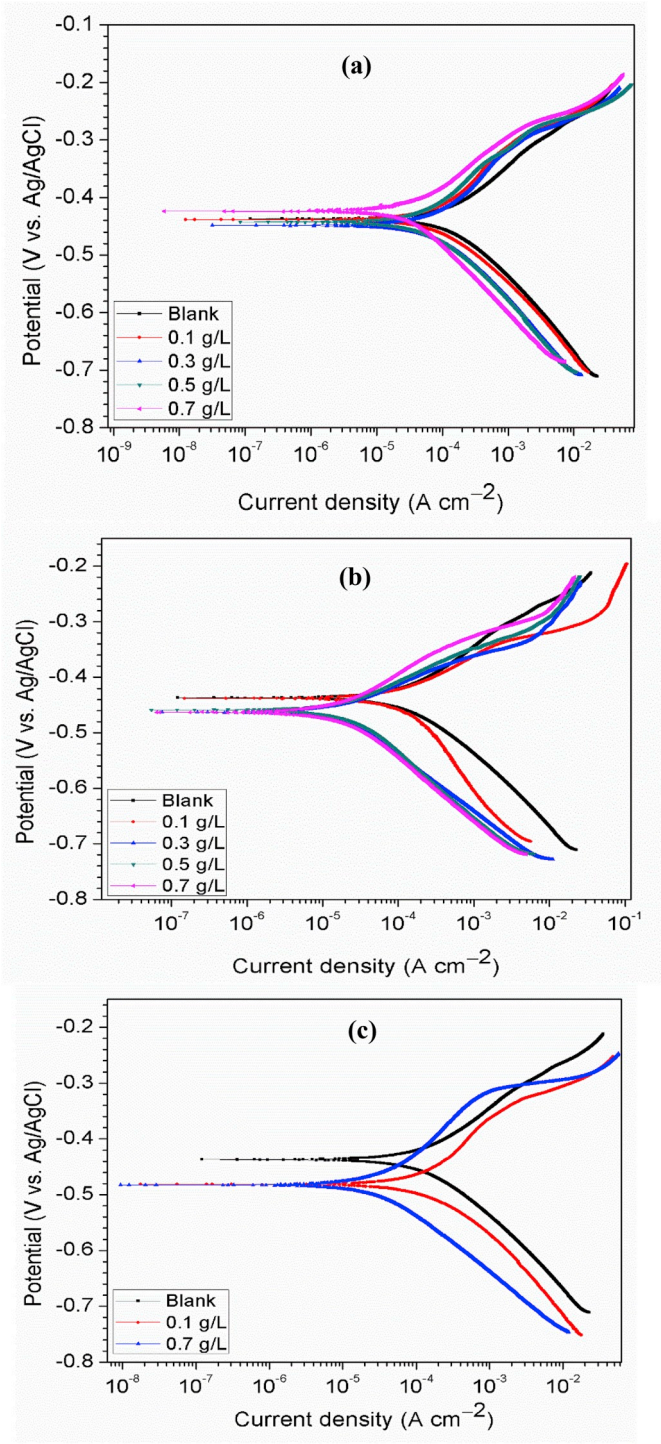

Fig. 5. Potentiodynamic polarization curves for low carbon steel in 1 moL/dm^3 HCl solution in the absence and presence of different concentrations of (a) aqueous, (b) ethanolic, and (c) methanolic *Pterocarpus santalinoides* extract at 25 °C.

anodic oxidation half corrosion reactions can be interrupted according to Eqs. (3) and (4) (Zhang and Hua, 2009; Gerengi et al., 2016). The FTIR results (Fig. 1) reveals that, PSLE extract contained compounds with –OH and –COOH functional groups. These groups could be protonated in HCl solution such that the extract molecules are adsorbed on the anodic site through columbic electrostatic attraction between positively charged molecules and $(FeCl^-)_{ads}$ steel surface (Zhang and Hua, 2009; Gerengi et al., 2016). On the other hand, protonated extract molecules could compete with H^+ ions on the cathodic site for adsorption (Yildiz et al., 2018). Such competitive adsorption had be reported (Yildiz et al., 2018; Kowsari et al., 2014).

$$Fe + Inh^+ \leftrightarrow Fe(Inh^+)_{ads} \quad (3)$$

$$Fe(Inh^+)_{ads} + e^- \leftrightarrow Fe(Inh)_{ads} \quad (4)$$

3.2.4. LPR studies

The dissolution behavior of low carbon steel in 1 moL/dm^3 HCl solution devoid of and containing PSLE extract was also examined by LPR technique. The data obtained from the inverse of the slope of the linear current versus potential graphs in the range of ±10 mV vs. OCP, since $R_p = dE/dj$ (Fernandes et al., 2019), where R_p is the polarization resistance, E is the potential (V) and j the current density (A cm^{-2}) are presented in Table 3. As noted in Table 3, higher R_p value is obtained in the fortified systems in comparison to the unprotected, meaning the steel dissolution was inhibited in the acid solution containing PSLE extract. As noted from other techniques, the corrosion inhibition performance of the extract is a function of concentration. From this technique, the presence of 0.7 g/L aqueous, ethanolic, and methanolic PSLE extract reduced the dissolution rate (v) of the substrate from 136.50 mpy to 33.68 mpy, 14.48 mpy, and 24.36 mpy, respectively. This may have been possible due to the adsorption of extract molecules on the electrode surface that raised the polarization resistance from 111.70 Ω cm^2 to 452.70 Ω cm^2, 811.40 Ω cm^2, and 627.60 Ω cm^2, respectively. The protection efficiency values obtained from the three electrochemical approaches (EIS, LPR, & PDP) are comparable (Table 2, Table 3).

3.3. The contribution of temperature to the corrosion inhibition by PSLE extract

To understand the contribution of temperature to the performance of PSLE extract towards inhibiting the deterioration of low carbon steel in 1 moL/dm^3 HCl environment, EIS, PDP, and LPR experiments were undertaken at 60 °C. This temperature was chosen since the temperature during chemical cleaning process rarely exceed 60 °C (Malik et al., 1997). Fig. 6 shows the EIS spectra and the PDP graphs obtained for the studied substrate in 1 moL/dm^3 HCl solution devoid of and containing 0.7 g/L PSLE extract at 60 °C. The associated electrochemical parameters are enumerated in Tables 4 and 5. It is certain from Fig. 6 and the results in Tables 4 and 5 that the extract effectively inhibited the corrosion of the low carbon steel in the studied medium. The diameter of the capacitive loop of the extract-inhibited graphs (Fig. 6(a)) is remarkably larger relative to that of the blank. More so, the impedance (Fig. 6(b)) and the Phase angle (Fig. 6(c)) are significantly displaced by the extract relative to the blank, and in the PDP graphs (Fig. 6(d)), the presence of the extract in the corrodent remarkably shifted the anodic and cathodic current densities to lower values in comparison to the blank.

By comparing the corrosion inhibition performance of PSLE extract at 25 °C (Tables 2 and 3) to its performance at 60 °C (Tables 4 and 5), it is found that the extract performed better at 60 °C. For instance, the corrosion inhibition efficiency of 0.7 g/L aqueous, ethanolic, and methanolic extract at 25 °C from EIS technique (Table 2) is 74.51%, 85.25%, and 72.38%, respectively but 94.80%, 92.86%, and 93.97% at 60 °C (Table 4). Similar trend is observed from the PDP and LPR techniques (Table 5). This observation suggest that, the extract molecules were chemically adsorbed on the steel surface (Gowraraju et al., 2007; Solomon et al., 2018), probably through the donation of electron pairs from O-heteroatoms in the extract molecules to the empty 3d-orbital of iron (Gowraraju et al., 2007; Solomon et al., 2018). As earlier mentioned, the –OH and –COOH functional groups on the extract molecules could be protonated in 1 moL/dm^3 HCl solution and adsorbed on the substrate surface through columbic attraction and/or competitive adsorption. On the surface, deprotonation could take place (Zarrouk

Table 3
Corrosion parameters for low carbon steel in 1 moL/dm^3 HCl solutions in the absence and presence of different concentrations of *Pterocarpus santalinoides* extract at 25 °C from potentiodynamic and linear polarization techniques.

Conc./System	Extracting solvent	PDP					LPR		
		$-E_{corr}$ (mV vs. Ag/AgCl)	i_{corr} (μA cm^{-2})	β_a (mV dec^{-1})	β_c (mV dec^{-1})	η_{PDP} (%)	R_p (Ω cm^2)	ν (mpy)	η_{LPR} (%)
Blank	–	436.45	124.25	101.20	111.40	–	111.70	136.50	–
0.1 g/L	Aqueous	438.29	71.65	128.30	105.30	42.33	207.60	73.46	46.19
0.3 g/L		447.71	60.57	119.00	113.30	51.25	241.70	60.09	53.79
0.5 g/L		441.57	41.02	107.30	101.50	66.99	332.60	45.85	66.42
0.7 g/L		423.98	30.25	86.90	115.10	75.65	452.70	33.68	75.33
0.1 g/L	Ethanolic	437.33	68.6	74.80	140.20	44.79	208.40	17.96	46.40
0.3 g/L		460.07	50.81	59.40	100.20	59.11	332.30	35.36	66.39
0.5 g/L		458.28	26.09	64.00	116.60	79.00	533.50	22.03	79.06
0.7 g/L		461.38	15.75	85.10	110.00	87.32	811.40	14.48	86.23
0.1 g/L	Methanolic	481.00	73.41	131.70	98.20	40.92	147.10	103.90	24.07
0.7 g/L		482.94	33.64	121.20	104.80	72.93	627.60	24.36	82.20

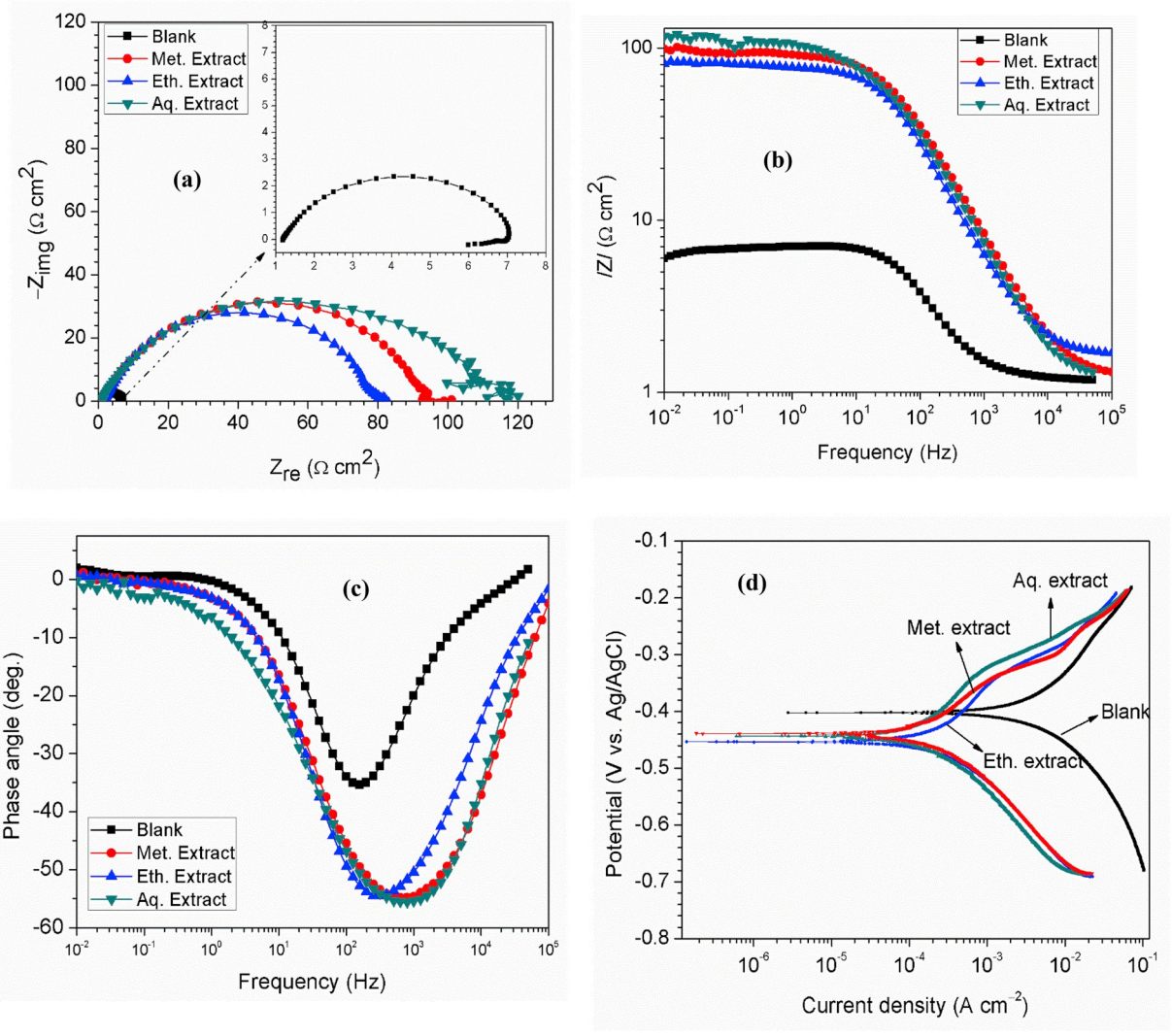

Fig. 6. Electrochemical impedance spectra for low carbon steel in 1 moL/dm^3 HCl solution in the absence and presence of 0.7 g/L PSLE extract at 60 °C in (a) Nyquist, (b) Bode modulus, and (c) Phase angle representations. (d) Potentiodynamic polarization curves for low carbon steel in 1 moL/dm^3 HCl solution in the absence and presence of 0.7 g/L PSLE extract at 60 °C.

et al., 2015; Solomon et al., 2018) such that some of the oxygen heteroatoms are freed (Zarrouk et al., 2015; Solomon et al., 2018). Electron pair could be transferred from the freed oxygen heteroatoms to the vacant 3d-orbital of Fe forming a covalent type of bond (Zarrouk et al., 2015; Solomon et al., 2018). The FTIR results (Fig. 1) also suggest that, the PSLE extract is rich in unsaturated organic compounds. The π-electrons from such compounds can as well be used for covalent bonding with Fe. As it is known, elevated temperatures favour this type of bonding (Zarrouk et al., 2015; Solomon et al., 2018).

To further elucidate the role of temperature on the dissolution behavior of the low carbon steel in the considered systems and to confirm the chemical interaction mechanism suggested by the variation

Table 4
Electrochemical impedance parameters for low carbon steel in 1 mol/dm^3 HCl solution in the absence and presence of 0.7 g/L PSLE extract at 60 °C.

Conc./ System	R_s (Ω cm^2)	CPE		R_{ct} (Ω cm^2)	x^2 × 10^{-3}	η_{EIS}
		Y_0 (μΩ^{-1} s^2 cm^{-2})	n			
Blank	1.21	1066.00	0.85	5.66	1.68	–
Eth. Extract	1.64	215.20	0.77	79.29	0.45	92.86
Aq. Extract	1.05	258.60	0.72	108.8	2.50	94.80
Meth. Extract	1.19	186.70	0.75	93.80	0.70	93.97

of protection efficiency with temperature, the apparent activation energy (E_a) for the corrosion process and the heat of adsorption (Q_{ads}) of the extract were calculated using Eqs. (5) and (6) (Solomon et al., 2017; Oguzie, 2007), respectively.

$$\log\frac{v_2}{v_1} = \frac{E_a}{2.303R}\left(\frac{1}{T_1}-\frac{1}{T_2}\right) \quad (5)$$

$$Q_{ads} = 2.303R\left[\log\left(\frac{\theta_2}{1-\theta_2}\right)-\log\left(\frac{\theta_1}{1-\theta_1}\right)\right]\times\left(\frac{T_1T_2}{T_2-T_1}\right)\ \text{kJmol}^{-1}$$

where v_1 and v_2 are the corrosion rates (derived from the LPR technique) at T_1 (25 °C) and T_2 (60 °C), respectively, θ_1 and θ_2 are the surface coverage (from LPR technique; $\theta = \eta/100$) at T_1 and T_2, respectively, R is the molar gas constant. The computed values of E_a and Q_{ads} are given in Table 6. In the table, the E_a value for both unprotected and protected systems is found to be positive and infers endothermic corrosion process (Solomon et al., 2017, 2018). However, the E_a values of the PSLE-fortified systems are smaller than that of the free corrodent. In the corrosion literature, such a behavior is common with chemical adsorption mechanism (Solomon et al., 2017, 2018; Oguzie, 2007). The Q_{ads} value calculated for the ethanolic, aqueous, and methanolic PSLE extract-inhibited systems is 16.88 kJ/mol, 46.49 kJ/mol, and 28.88 kJ/mol, respectively. The Q_{ads} values are all positive and is a characteristic of a chemisorption mechanism (Oguzie, 2007; Solomon et al., 2017), thus confirms that the PSLE extract chemically adsorbed onto the low carbon steel surface in 1 moL/dm^3 HCl medium.

3.4. Comparison of the protection efficacy of PSLE extract from different extractive solvents

It is a fact that extractive solvents differ in extraction preference and strength. For instance, Anokwuru et al. (2011) reported that, ethanol had the ability to extract flavonoids and phenolics in the bark of *Azadirachta indica* than absolute methanol, ethyl acetone, and acetone. Similarly, Umoren et al. (2014) reported that, ethanol extracted polyphenols and flavonoids from coconut coir dust more than acetone. These differences in extraction preference and strength could have effect on the dissolution inhibition performance of a plant extract. To study the effect of extractive solvent on the dissolution inhibition performance by PSLE extract, water, ethanol, and methanol were used for extraction. The values of inhibition efficiency of PSLE extract obtained from the various applied techniques are given in Table 7. The data in the table disclose that, the extractive solvent has effect on the corrosion inhibition performance of the extract. On the average, the order of corrosion inhibition performance by the PSLE extract is ethanolic > methanolic > aqueous. This result could be associated with the phytochemical constituents of the *Pterocarpus santalinoides* leaves extracted by the solvents. Going by the report of Bothon et al. (2014), ethanol has a higher efficacy of extracting tannin and flavonoid contents from *Pterocarpus santalinoides* leaves than water. It had been documented that tannins are excellent corrosion inhibitor for carbon steel due to their ability to form a highly cross-linked network of ferric tannate moieties (Oguzie, 2008; Umoren et al., 2014). Nevertheless, since the extract is a multi-component as revealed by the FTIR spectra (Fig. 1), the other phytochemical constituents could equally chelate with ferric ions and facilitate strong adsorption on the steel surface. The overall corrosion inhibition may possibly be a synergistic interaction between the different adsorbed constituents (Umoren et al., 2014, 2019).

3.5. Proposed mechanism of inhibition by PSLE extract

The calculated values of E_a and Q_{ads} (Table 7) suggested that, PSLE extract adsorbed onto the low carbon steel surface through chemical adsorption mechanism. Such adsorption mode would result in Fe-extract complex formation. To confirm the formation of Fe-extract complex and to propose a mechanism for the corrosion inhibition of low carbon steel corrosion in 1 moL/dm^3 HCl solution by PSLE extract, UV–vis experiments were undertaken. The UV–vis spectra obtained for 1 moL/dm^3 HCl solution containing ethanolic PSLE extract (a) before and (b) after low carbon steel sample immersion for 24 h at room temperature are presented in Fig. 7. The spectrum in Fig. 7(a) exhibits two bands at 212 nm and 422 nm and are assigned to the π→π* and n→π* electronic transitions, respectively (Saxena et al., 2018c, 2018a, 2018b; Sanaei et al., 2019). In contrast, the spectrum in Fig. 7(b) showed additional band at 333 nm and this is indicative of Fe-extract complex formation. Similar submission can be found in the literature (Alvarez et al., 2018; Haladu et al., 2019). Further inspection of Fig. 7 reveals that, the

Table 6
Calculated values of kinetic parameters for low carbon steel in 1 moL/dm^3 HCl solution in the absence and presence of 0.7 g/L PSLE extract.

System	E_a (kJ/mol)	Q_{ads} (kJ/mol)
Blank	71.52	–
Ethanolic extract	62.52	16.88
Aqueous extract	30.67	46.49
Methanolic extract	45.75	28.88

Table 7
Comparison of inhibition efficiencies of *Pterocarpus santalinoides* extracts obtained from different extractive solvents.

System	Inhibition efficiency (%)			
	EIS	PDP	LPR	Average
Aqueous extract	74.51	75.65	75.33	75.16
Ethanolic extract	76.94	87.32	86.23	83.50
Methanolic extract	72.38	72.93	82.20	75.84

Table 5
Corrosion parameters for low carbon steel in 1 moL/dm^3 HCl solutions in the absence and presence of 0.7 g/L PSLE extract at 60 °C from potentiodynamic polarization.

Conc./System	PDP					LPR		
	E_{corr} (mV vs. Ag/AgCl)	i_{corr} (μA cm^{-2})	β_a (mV dec^{-1})	β_c (mV dec^{-1})	η_{PDP} (%)	R_p (Ω cm^2)	v (mpy)	η_{LPR} (%)
Blank	401.10	4563.54	188.10	145.40	–	5.60	2835.00	–
Eth. Extract	452.62	220.46	150.40	109.40	95.17	77.31	205.30	92.76
Aq. Extract	442.51	114.48	134.60	95.30	97.49	128.30	123.70	95.64
Meth. Extract	437.70	138.36	108.70	93.60	96.97	93.61	169.60	94.02

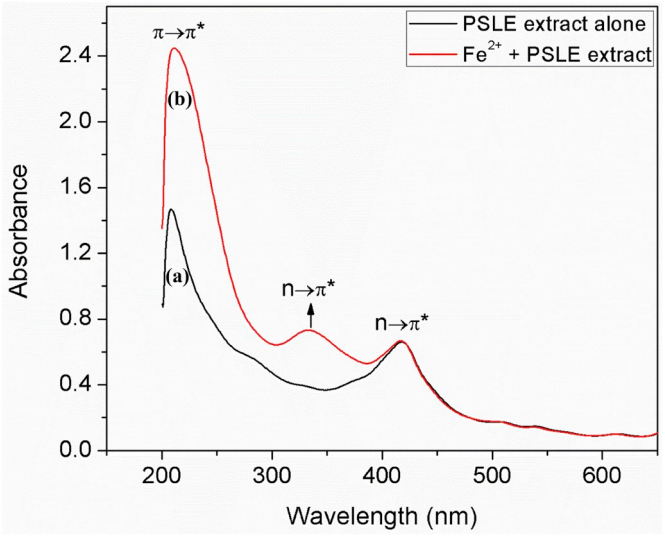

Fig. 7. UV–visible spectra of the extract of ethanolic *Pterocarpus santalinoides* extract in 1 moL/dm^3 HCl before and after immersion of low carbon steel sample.

adsorption process affected the band at 212 nm, i.e. higher intensity in Fig. 7(b) than in Fig. 7(a). As it is known, a sharp absorbance band at around 200–215 nm is consistent with the hydroxide functionality (Zuman and Szafranski, 1976). This suggests that, the O–H functional groups on the extract phytochemical compounds participated in the adsorption process.

The inhibition of the low carbon steel corrosion in the studied corrosive medium by PSLE extract can therefore be explained by virtue of adsorption mechanism. The PSLE extract is rich in organic compounds bearing O–H groups (Fig. 1). The O–H functional groups can be protonated in 1 moL/dm^3 HCl solution such that the extract active compounds exist in cationic forms (Obot et al., 2019). The adsorption of the cationic inhibitor species on the substrate surface would depend on the metal surface charge. The net charge (φ) on the carbon steel surface can be ascertained using the following equation (Mobin et al., 2019): $E_{corr} - E_{zpc} = \varphi$, where E_{corr} is corrosion potential and E_{zpc} is the potential of zero charge. Pavithra et al. (2016) reported − 498 mV vs. Ag/AgCl as the E_{zpc} for low carbon steel in 1 moL/dm^3 HCl solution. From our result (Table 4), the E_{corr} for the studied carbon steel is − 436 mV vs. Ag/AgCl. Since the difference between E_{corr} and E_{zpc} (+62 mV vs. Ag/AgCl) is greater than zero, the low carbon steel surface in 1 moL/dm^3 HCl solution would be positively charged (Mobin et al., 2019). Obviously, chloride (Cl^-) ions would be adsorbed on the surface and the adsorption would replenish the surface (Mobin et al., 2019; Haladu et al., 2019) to favour the adsorption of the protonated inhibitor species through electrostatic attraction (Physisorption mechanism). On the surface, lone pair of electrons from O-heteroatom of the inhibitor molecules may have been transferred into the d-orbital of Fe to form Fe-extract complex (hence, the chemisorption mechanism) as indicated by the UV–vis results.

3.6. Surface observation studies

3.6.1. SEM and EDAX studies

The surfaces of the corroded low carbon steel specimens after immersion in 1 moL/dm^3 HCl solution without and with 0.7 g/L aqueous, ethanolic, and methanolic PSLE extract for 24 h at 25 °C was examined using SEM-EDAX techniques. The SEM images and the corresponded EDAX spectra obtained from the examination are presented in Fig. 8. In the absence of PSLE extract, the SEM picture (Fig. 8(a)) reveals a severe attack on the steel surface in the acidic solution. A rough morphology is observed in the image shown in Fig. 8(a). The EDAX spectrum reported

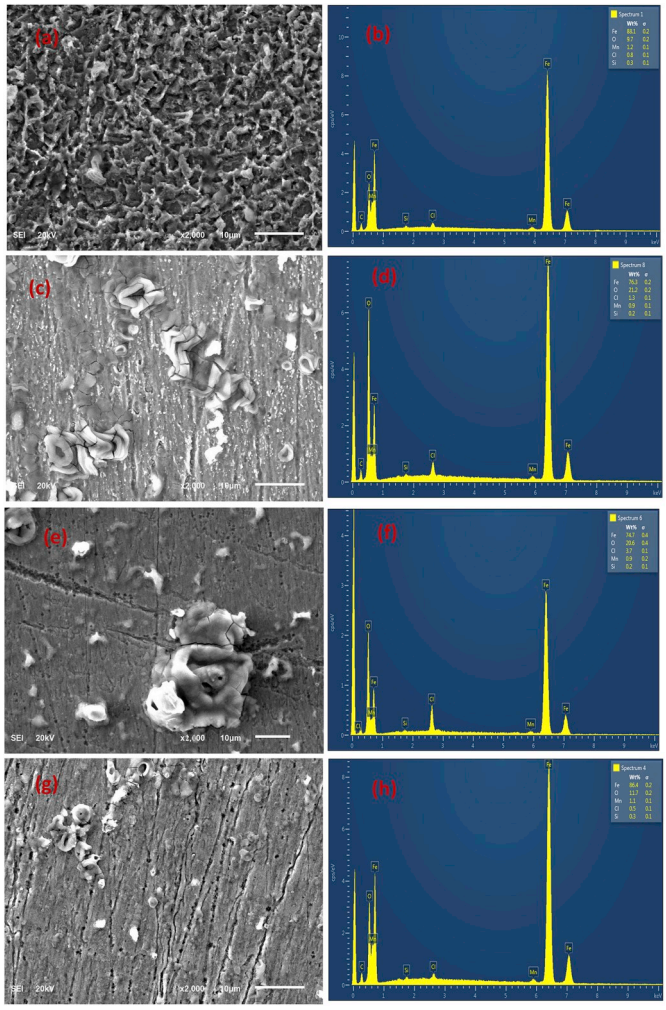

Fig. 8. SEM images and EDAX spectra of a low carbon steel coupon immersed in 1 moL/dm^3 HCl solution (a, b) without and with (c, d) Aqueous, (e,f) methanolic, and (g, h) ethanolic *Pterocarpus santalinoides* extract for 24 h at ordinary temperature.

in Fig. 8(b) shows Cl and O peaks in addition to the characteristic peaks of the carbon steel specimen, indicating the presence of oxides and chlorides in the corrosion products (Solomon et al., 2019). It can be seen in the inserted table in Fig. 8(b) that the weight percentage of O on the surface of the corroded sample (Fig. 8(a)) is 9.7%. By comparing the micrographs of the PSLE extract-inhibited surfaces (Fig. 8(c, e, g)) to that of the blank (Fig. 8(a)), the images in Fig. 8(c, e, g) are smoother than the image in Fig. 8(a). This confirms the corrosion inhibition of the studied substrate by the PSLE extract. The EDAX spectra in Fig. 8(d, f, g) reveals an increment in the content of oxygen species from 9.7% (Fig. 8 (b)) to 21.2% (Fig. 8(d)), 20.6% (Fig. 8(f)), and 11.7% (Fig. 8(g)) on the specimen surfaces exposed to the acid solution inhibited with PSLE extract. This result confirms the adsorption of PSLE molecules on the specimen surface. The adsorbed molecules protected the surface from corrosion as reveals by the experimental results (Tables 3 and 4) and the SEM images (Fig. 8(c, e, g)).

3.6.2. AFM studies

In Fig. 9 is presented the 2D and 3D AFM pictures taken for the low carbon steel specimen after exposing to 1 moL/dm^3 HCl solution devoid of and containing 0.7 g/L ethanolic PSLE extract for 24 h at room temperature. The graphs showing the surface roughness profile as well as the associated roughness parameters as contained in the International Organization of Standardization (ISO) 1487 are also presented. The

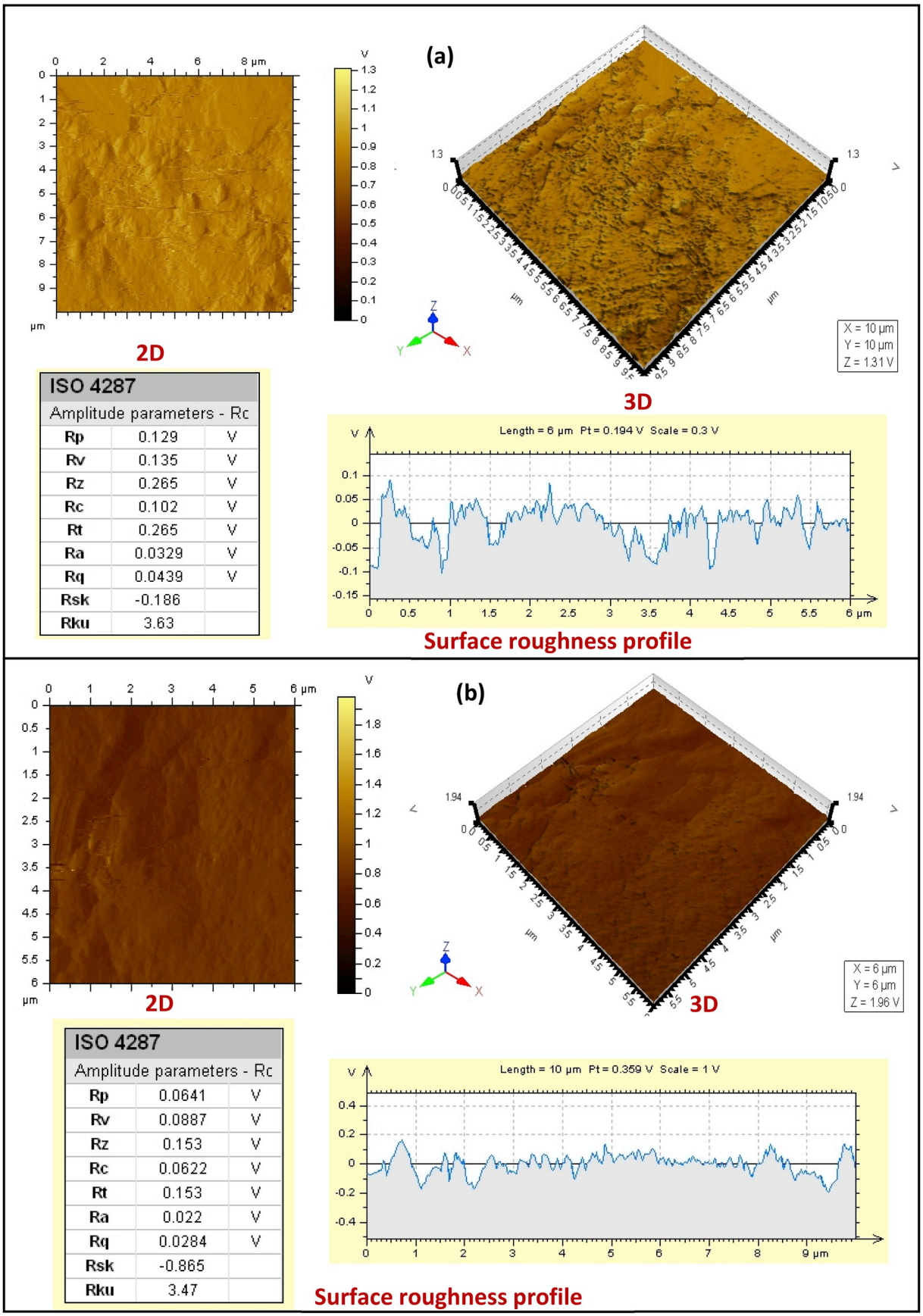

Fig. 9. AFM images in of a low carbon steel coupon immersed in 1 moL/dm^3 HCl solution (a) without and (b) with 0.7 g/L ethanolic PSLE extract for 24 h at ordinary temperature.

definition of the parameters are given elsewhere (Solomon et al., 2018). Clearly, the surface in Fig. 9(b) is smoother compare to the one in Fig. 9 (a). The values of all the roughness parameters in Fig. 9(b) are smaller than those in Fig. 9(a). Again, there are more deeply penetrated pits in the surface profile graph in Fig. 9(a) than in Fig. 9(b). All these indicate less corrosion of the studied substrate in the PSLE-inhibited acid solution than in the unprotected acid solution and is in conformity with results from other applied techniques.

3.7. Conclusions

In this article, the crude extract of *Pterocarpus santalinoides* (PSLE) is shown to be an effective in suppressing the dissolution of low carbon steel in 1 moL/dm^3 HCl solution. The results obtained from EIS, PDP, and LPR corroborate each other. The protection efficacy of PSLE gets better with increase in dosage and temperature. With 0.7 g/L PSLE, the surface of the studied substrate has be protected by over 90% at 60 °C. It is proposed from the calculated values of E_a, Q_{ads}, and UV–vis results that, PSLE molecules chemically interacted with the steel surface. PSLE extract behaves a mixed type corrosion inhibitor according to the PDP results. However, aqueous PSLE extract has dominant effect on the anodic corrosion reactions while ethanolic and methanolic extracts have primary effect on the cathodic corrosion reactions. The order of protection efficacy by the different solvent extracts is ethanolic extract > methanolic extract > aqueous extract. Surface characterization results via SEM, EDAX, and AFM are in support of the claim of adsorption of PSLE molecules on the studied substrate surface.

Declaration of competing interest

The authors declare that they have no known competing financial interests or personal relationships that could have appeared to influence the work reported in this paper.

Acknowledgements

The authors are grateful to the Center of Research Excellence in Corrosion, Research Institute, King Fahd University of Petroleum and Minerals, Saudi Arabia for granting permission for some of its equipment to be used in this work.

Appendix A. Supplementary data

Supplementary data to this article can be found online at https://doi.org/10.1016/j.scp.2019.100196.

References

Alibakhshi, E., Ramezanzadeh, M., Haddadi, S.A., Bahlakeh, G., Ramezanzadeh, B., Mahdavian, M., 2019. *Persian Liquorice* extract as a highly efficient sustainable corrosion inhibitor for mild steel in sodium chloride solution. J. Clean. Prod. 210, 660–672.

Alvarez, P.E., Fiori-Bimbi, M.V., Neske, A., Brandán, S.A., Gervasi, C.A., 2018. *Rollinia occidentalis* extract as green corrosion inhibitor for carbon steel in HCl solution. J. Ind. Eng. Chem. 58, 92–99.

Anokwuru, C.P., Anyasor, G.N., Ajibaye, O., Fakoya, O., Okebagwu, P., 2011. Effect of extraction solvents on phenolic, flavonoids and antioxidant activities of three Nigerian medicinal. Nat. Sci. 9, 53–61.

Asadi, N., Ramezanzadeh, M., Bahlakeh, G., Ramezanzadeh, B., 2019. Utilizing *Lemon Balm* extract as an effective green corrosion inhibitor for mild steel in 1M HCl solution: a detailed experimental, molecular dynamics, Monte Carlo and quantum mechanics study. J. Taiwan Inst. Chem. Eng. 95, 252–272.

Ashassi-Sorkhabi, A., Majidi, M.R., Seyyedi, K., 2004. Investigation of inhibition effect of some amino acids against steel corrosion in HCl solution. Appl. Surf. Sci. 225, 176–185.

Ashassi-Sorkhabi, H., Ghalebsaz-Jeddi, N., Hashemzadeh, F., Jahani, H., 2006. Corrosion inhibition of carbon steel in hydrochloricacid by some polyethylene glycols. Electrochim. Acta 51, 3848–3854.

ASTM G3-89, 1994. Conventions Applicable to Electrochemical Measurements in Corrosion Testing, vol. 30. Annual Book of ASTM standard.

ASTM G3-94, 1994. Making Potentiostatic and Potentiodynamic Anodic Polarization Measurements, vol. 48. Annual Book of ASTM standard.

Bahlakeh, G., Ramezanzadeh, B., Dehghani, A., Ramezanzadeh, M., 2019. Novel cost-effective and high-performance green inhibitor based onaqueous *Peganum harmala* seed extract for mild steel corrosion in HCl solution: detailed experimental and electronic/atomic level computational explorations. J. Mol. Liq. 283, 174–195.

Bahlakeh, G., Dehghani, A., Ramezanzadeh, B., Ramezanzadeh, M., 2019. Highly effective mild steel corrosion inhibition in 1 M HCl solution by novel green aqueous Mustard seed extract: experimental, electronic-scale DFT and atomic-scale MC/MD explorations. J. Mol. Liq. 293, 111559.

Benarioua, M., Mihi, A., Bouzeghaia, N., Naoun, M., 2019. Mild steel corrosion inhibition by Parsley (*Petroselium Sativum*) extract in acidic media. Egypt. J. Pet. 28, 155–159.

Bhardwaj, N., Prasad, D., Haldhar, R., 2018. Study of the *Aegle marmelos* as a green corrosion inhibitor for mild steel in acidic medium: experimental and theoretical approach. J. Bio- and Tribo-Corros. 4 (61), 1–10.

Bothon, F.T.D., Moustapha, M., Bogninou, G.S., Agbangnan Dossa, C.P., Yehouenou, B., Medoatinsa, S.E., Noudogbessi, J.P., Avlessi, F., Sohounhloue, D.C.K., 2014. Chemical characterization and biological activities of *Newbouldia laevis* and *Pterocarpus Santalinoides* leaves. Bull. Environ. Pharmacol. Life Sci. 3 (11), 09–15.

Brug, G.J., van den Eeden, A.L.G., Rehbach, M.S., Sluyters, J.H., 1984. The analysis of electrode impedances complicated by the presence of a constant phase element. J. Electroanal. Chem. Interfacial Electrochem. 176, 275–295.

Chellouli, L.M., Chebabe, D., Dermaj, A., Erramli, H., Bettach, N., Hajjaji, N., Casaletto, M.P., Cirrincione, C., Privitera, A., Srhiri, A., 2016. Corrosion inhibition of iron in acidic solution by a green formulation derived from *Nigella sativa*. Electrochim. Acta 204, 50–59.

Dehghani, A., Bahlakeh, G., Ramezanzadeh, B., Ramezanzadeh, M., 2019. Potential of *Borage* flower aqueous extract as an environmentally sustainable corrosion inhibitor for acid corrosion of mild steel: electrochemical and theoretical studies. J. Mol. Liq. 277, 895–911.

Dehghani, A., Bahlakeh, G., Ramezanzadeh, B., 2019. Green *Eucalyptus* leaf extract: a potent source of bio-active corrosion inhibitors for mild steel. Bioelectrochemistry 130, 107339.

Dehghani, A., Bahlakeh, G., Ramezanzadeh, B., 2019. A detailed electrochemical/theoretical exploration of the aqueous *Chinese gooseberry* fruit shell extract as a green and cheap corrosion inhibitor for mild steel in acidic solution. J. Mol. Liq. 282, 366–384.

Dehghani, A., Bahlakeh, G., Ramezanzadeh, B., Ramezanzadeh, M., 2019. A combined experimental and theoretical study of green corrosion inhibition of mild steel in HCl solution by aqueous *Citrullus lanatus* fruit(CLF) extract. J. Mol. Liq. 279, 603–624.

Fang, Y., Suganthan, B., Ramasamy, R.P., 2019. Electrochemical characterization of aromatic corrosion inhibitors from plant extracts. J. Electroanal. Chem. 840, 74–83.

Fernandes, C.M., Fagundes, T.S.F., dos Santos, N.E., de, M., Rocha, T.S., Garrett, R., Borges, R.M., Muricy, G., Valverde, A.L., Ponzio, E.A., 2019. *Ircinia strobilina* crude extract as corrosion inhibitor for mild steel in acid medium. Electrochim. Acta 312, 137–148.

Gerengi, H., Ugras, H.I., Solomon, M.M., Umoren, S.A., Kurtay, M., Atar, N., 2016. Synergistic corrosion inhibition effect of 1-ethyl-1-methylpyrrolidinium tetrafluoroborate and iodide ions for low carbon steel in HCl solution. J. Adhes. Sci. Technol. 30, 2383–2403.

Gowraraju, N.D., Jagadeesan, S., Ayyasamy, K., Olasunkanmi, L.O., Ebenso, E.E., Subramanian, C., 2007. Adsorption characteristics of iota-carrageenan and inulin biopolymers as potential corrosion inhibitors at mild steel/sulphuric acid interface. J. Mol. Liq. 232, 9–19.

Haladu, S.A., Umoren, S.A., Ali, S.A., Solomon, M.M., Mohammed, A.I., 2019. Synthesis, characterization and electrochemical evaluation of anticorrosion property of a tetrapolymer for carbon steel in strong acid media. Chin. J. Chem. Eng. 27, 965–978.

Haldhar, R., Prasad, D., Saxena, A., 2018. *Myristica fragrans* extract as an eco-friendly corrosion inhibitor for mild steel in 0.5M H_2SO_4 solution. J. Environ. Chem. Eng. 6, 2290–2301.

Haldhar, R., Prasad, D., Saxena, A., 2018. *Armoracia rusticana* as sustainable and eco-friendly corrosion inhibitor for mild steel in 0.5M sulphuric acid: experimental and theoretical investigations. J. Environ. Chem. Eng. 6, 5230–5238.

Haldhar, R., Prasad, D., Saxena, A., Kumar, R., 2018. Experimental and theoretical studies of *Ficus religiosa* as green corrosion inhibitor for mild steel in 0.5M H2SO4 solution. Sustain. Chem. Pharm. 9, 95–105.

Igoli, J.O., Ogaji, O.G., Tor, A.A., Igoli, N.P., 2005. Traditional medicinal practice amongst the Igede people of Nigeria, Part II. Afr. J. Tradit., Complementary Altern. Med. 2 (2), 134–152.

Kannan, P., Karthikeyan, J., Murugan, P., Rao, T.S., Rajendran, N., 2016. Corrosion inhibition effect of novel methyl benzimidazolium ionic liquid for carbon steel in HCl medium. J. Mol. Liq. 221, 368–380.

Kowsari, M., Payami, R., Amini, B., Ramezanzadeh, M., Javanbakh, E., 2014. Task-specific ionic liquid as a new green inhibitor of mild steel corrosion. Appl. Surf. Sci. 289, 478–486.

Luo, X., Ci, C., Li, J., Lin, K., Du, S., Zhang, H., Li, X., Cheng, Y.F., Zang, J., Liu, Y., 2019. 4-aminoazobenzene modified natural glucomannan as a green eco-friendly inhibitor for the mild steel in 0.5 M HCl solution. Corros. Sci. 151, 132–142.

Malik, A.U., Ahmad, S., Andijani, I., Asrar, N., 1997. Acid Cleaning of Some Desal Units at Al-Jubail Plant. Technical Report No. TR3804/APP95007.

Mansfeld, F., Tsai, C.H., Shih, H., 1992. In: Munn, R.S. (Ed.), Computer Modeling in Corrosion. ASTM, Philadelphia, PA, p. 86.

Mobin, M., Basik, M., Aslam, J., 2019. Pineapple stem extract (*Bromelain*) as an environmental friendly novel corrosion inhibitor for low carbon steel in 1 M HCl. Measurement 134, 595–605.

Nikpour, S., Ramezanzadeh, M., Bahlakeh, G., Ramezanzadeh, B., Mahdavian, M., 2019. *Eriobotrya japonica* Lindl leaves extract application for effective corrosion mitigation of mild steel in HCl solution: experimental and computational studies. Construct. Build. Mater. 220, 161–176.

Noor, E.A., 2005. The inhibition of mild steel corrosion in phosphoric acid solutions by some N-heterocyclic compounds in the salt form. Corros. Sci. 47, 33–55.

Obot, I.B., Onyeachu, I.B., Kumar, A.M., 2017. Sodium alginate: a promising biopolymer for corrosion protection of API X60 high strength carbon steel in saline medium. Carbohydr. Polym. 178, 200–208.

Obot, I.B., Onyeachu, I.B., Nuha, W., Al-Amri, A.H., 2019. Theoretical and experimental investigation of two alkyl carboxylates as corrosion inhibitors for steel in acidic medium. J. Mol. Liq. 279, 190–207.

Ofoma, E.O., Ekemezie, P.N., Emeruwa, C.N., 2018. Mild steel deterioration inhibition in 1.0 M and 5.0 M tetraoxosulphate (VI) acid using leaf extract of *Pterocarpus santaliniodes*. J. Appl. Sci. Environ. Manag. 22 (8), 1337–1341.

Oguzie, E.E., 2007. Corrosion inhibition of aluminium in acidic and alkaline media by *Sansevieria trifasciata* extract. Corros. Sci. 49, 1527–1539.

Oguzie, E.E., 2008. Evaluation of the inhibitive effect of some plant extracts on the acid corrosion of mild steel. Corros. Sci. 50, 2993–2998.

Oguzie, E.E., Li, Y., Wang, F.H., 2007. Corrosion inhibition and adsorption behavior of methionine on mild steel in sulphuric acid and synergistic effect of iodide ion. J. Colloid Interface Sci. 310, 90–98.

Okwuosa, C.N., Unekwe, P.C., Achukwu, P.U., Udeani, T.K.C., Ogidi, U.H., 2011. Glucose and triglyceride lowering activity of *Pterocarpussantaniloides* leaf extracts against dexamethasone induced hyperlipidemia and insulin resistance in rats. Afr. J. Biotechnol. 10 (46), 9415–9420.

Osuagwu, G.G.E., Akomas, C.B., 2013. Antimicrobial activity of the leaves of three species of Nigerian *Pterocarpus*(Jacq.). Int. J. Med. Aromatic Plants 3 (2), 178–183.

Otzisk, B., 2008. Chemical cleaning and degassing refinery equipment. PTQ Q1 77, 81.

Pavithra, M.K., Venkatesha, T.V., Punith Kumar, M.K., Anantha, N.S., 2016. Electrochemical, gravimetric and quantum chemical analysis of mild steel corrosion inhibition by colchicine in 1 M HCl medium. Res. Chem. Intermed. 42, 2409–2428.

Sanaei, Z., Bahlakeh, G., Ramezanzadeh, B., Ramezanzadeh, M., 2019. Application of green molecules from *Chicory* aqueous extract for steel corrosion mitigation against chloride ions attack; the experimental examinations and electronic/atomic level computational studies. J. Mol. Liq. 290, 111176.

Satapathy, A.K., Gunasekaran, G., Sahoo, S.C., Amit, K., Rodrigues, P.V., 2009. Corrosion inhibition by *Justicia gendarussa* plant extract in hydrochloric acid solution. Corros. Sci. 51, 2848–2856.

Saxena, A., Prasad, D., Haldhar, R., 2018. Investigation of corrosion inhibition effect and adsorption activities of *Cuscuta reflexa* extract for mild steel in 0.5 M H_2SO_4. Bioelectrochemistry 124, 156–164.

Saxena, A., Prasad, D., Haldhar, R., 2018. Use of *Asparagus racemosus* extract as green corrosion inhibitor for mild steel in 0.5 M H2SO4. J. Mater. Sci. 53, 8523–8535.

Saxena, A., Prasad, D., Haldhar, R., Singh, G., Kumar, A., 2018. Use of *Saraca ashoka* extract as green corrosion inhibitor for mild steel in 0.5 M H_2SO_4. J. Mol. Liq. 258, 89–97.

Sigircik, G., Tüken, T., Erbil, M., 2016. Assessment of the inhibition efficiency of 3, 4-diaminobenzonitrile against the corrosion of steel. Corros. Sci. 102, 437–445.

Solomon, M.M., Umoren, S.A., 2016. In-situ preparation, characterization and anticorrosion property of polypropylene glycol/silver nanoparticles composite for mild steel corrosion in acid solution. J. Colloid Interface Sci. 462, 29–41.

Solomon, M.M., Gerengi, H., Kaya, T., Umoren, S.A., 2017. Performance evaluation of a chitosan/silver nanoparticles composite on St37 steel corrosion in a 15% HCl solution. ACS Sustain. Chem. Eng. 5, 809–820.

Solomon, M.M., Umoren, S.A., Obot, I.B., Sorour, A.A., Gerengi, H., 2018. Exploration of dextran for application as corrosion inhibitor for steel in strong acid environment: effect of molecular weight, modification, and temperature on efficiency. ACS Appl. Mater. Interfaces 10, 28112–28129.

Solomon, M.M., Umoren, S.A., Quraishi, M.A., Salman, M., 2019. Myristic acid based imidazoline derivative as effective corrosion inhibitor for steel in 15% HCl medium. J. Colloid Interface Sci. 551, 47–60.

Srikanth, A.P., Sunitha, T.G., Raman, V., Nanjundan, S., Rajendran, N., 2007. Synthesis, characterization and corrosion protection properties of poly (n-(acryloyloxymethyl) benzotriazole-co-glycidyl methacrylate) coatings on mild steel. Mater. Chem. Phys. 103, 241–247.

Tuken, T., Demir, F., Kıcır, N., Sıgırcık, G., Erbil, M., 2012. Inhibition effect of 1-ethyl-3-methylimidazolium dicyanamide against steel corrosion. Corros. Sci. 59, 110–118.

Umoren, S.A., Solomon, M.M., Eduok, U.M., Obot, I.B., Israel, A.U., 2014. Inhibition of mild steel corrosion in H_2SO_4 solution by coconut coir dust extract obtained from different solvent systems and synergistic effect of iodide ions: ethanol and acetone extracts. J. Environ. Chem. Eng. 2, 1048–1060.

Umoren, S.A., Solomon, M.M., Obot, I.B., Suleiman, R.K., 2019. A critical review on the recent studies on plant biomaterials as corrosion inhibitors for industrial metals. J. Ind. Eng. Chem. 76, 91–115.

Wang, Q., Tan, B., Bao, H., Xie, Y., Mou, Y., Li, P., Chen, D., Shi, S., Li, X., Yang, W., 2019. Evaluation of *Ficus tikoua* leaves extract as an eco-friendly corrosion inhibitor for carbon steel in HCl media. Bioelectrochemistry 128, 49–55.

World Agroforestry Centre, 2008. Agro Forestry Tree Database – Pterocarpus Santalinoides.

Yildiz, M., Gerengi, H., Solomon, M.M., Kaya, E., Umoren, S.A., 2018. Influence of 1-butyl-1-methylpiperidinium tetrafluoroborate on St37 steel dissolution behavior in HCl environment. Chem. Eng. Commun. 205, 538–548.

Zarrouk, A., Hammouti, B., Lakhlifi, T., Traisnel, M., Vezin, H., Bentiss, F., 2015. New 1H-pyrrole-2,5-dione derivatives as efficient organic inhibitors of carbon steel corrosion in hydrochloric acid medium: electrochemical, XPS and DFT studies. Corros. Sci. 90, 572–584.

Zhang, Q.B., Hua, Y.X., 2009. Corrosion inhibition of mild steel by alkylimidazolium ionic liquids in hydrochloric acid. Electrochim. Acta 54, 1881–1887.

Zhao, Y., Pan, T., Yu, X., Chen, D., 2019. Corrosion inhibition efficiency of triethanolammonium dodecylbenzene sulfonate on Q235 carbon steel in simulated concrete pore solution. Corros. Sci. 158, 108097.

Zohdy, K.M., 2015. Surface protection of carbon steel in acidic solution using ethylenediamine tetraacetic disodium salt. Int. J. Electrochem. Sci. 10, 414.

Zuman, P., Szafranski, W., 1976. Ultraviolet spectra of hydroxide, alkoxide, and hydrogen sulfide anions. Anal. Chem. 48 (1), 2162 – 21.